

Düzce University Journal of Science & Technology

Research Article



Gas Metal Arc Weldability of Ramor 500 Ballistic Armor Steels

D Hayriye ERTEK EMRE a,*, D Serkan KEÇE a, D Ramazan KAÇAR a

^a Department of Manufacturing Engineering, Faculty of Technology, Karabük University, Karabük, TÜRKİYE

* Corresponding author's e-mail address: hayriyeertek@karabuk.edu.tr DOI: 10.29130/dubited.1624262

ABSTRACT

Ramor 500 armor steel is classified as high strength ballistic protection steel produced in the hardness range 490-506 HB. They are preferred and used in armored vehicle manufacturing due to their high hardness, resistance to ballistic explosions and abrasion. Armored military vehicles are frequently subjected to impact and dynamics loads. Therefore, mechanical properties of armor steel and their weldment must be determined. In this study, Ramor 500 armor steels were joined by gas metal arc welding, (GMAW), method. The weldments were subjected to a radiographic examination by X-ray radiographic inspection method. Tensile, Charpy V notch-impact and bending tests were carried out for determining the mechanical properties of the weldment. The fractures of tensile test sample were analyzed by scanning electron microscopy. The microstructural examinations of the weldments were also carried out and hardness distributions were determined. Results confirm that the Ramor 500 armor steels have been successfully joined by the automated GMAW method. The strength and ductility of the joints are found within the acceptable range. The weld metal impact notch absorption energy of the GMAW joint was found to be higher than the base metal. However, the weld metal strength was found to be lower than the base metal. The lowest hardness of the weldment is determined in the HAZ next to the base metal due to softening.

Keywords: Ramor 500 armor steel, GMAW, weldability, mechanical properties, fracture type

Ramor 500 Balistik Zırh Çeliklerinin Gaz Metal Ark Kaynağı ile Birleştirilebilirliği



Ramor 500 zırh çeliği 490-506 HB sertlik aralığında üretilen yüksek mukavemetli balistik koruma çeliği olarak sınıflandırılır. Yüksek sertlikleri, balistik patlamalara ve aşınmaya karşı dirençleri nedeniyle zırhlı araç imalatında tercih edilir ve kullanılırlar. Zırhlı askeri araçlar sıklıkla darbeye ve dinamik yüklere maruz kalmaktadır. Bu nedenle zırh çeliğinin ve kaynaklı birleştirmelerinin mekanik özelliklerinin belirlenmesi gerekmektedir. Bu çalışmada, Ramor 500 zırh çelikleri gaz altı ark kaynak (GMAK) yöntemi ile birleştirilmiştir. Kaynaklı birleştirmeler X-ışını radyografik muayene yöntemi ile radyografik incelemeye tabi tutulmuştur. Birleştirmelerin mekanik özelliklerini belirlemek için çekme, Charpy-V çentik darbe ve eğme testleri yapılmıştır. Çekme testi numunelerinin kırılma yüzeyleri taramalı elektron mikroskobu (SEM) ile incelenmiştir. Birleştirmelerin mikroyapı incelemeleri de gerçekleştirilerek, sertlik dağılımları belirlenmiştir. Sonuçlar, Ramor 500 zırh çeliklerinin GMAK yöntemiyle başarılı bir şekilde birleştirilebildiğini doğrulamaktadır. Birleştirmelerin dayanım ve sünekliği kabul edilebilir aralıkta bulunmuştur. GMAK birleştirmesinin kaynak metali çentik darbe emme enerjisi ana metalden daha yüksek bulunmuştur. Fakat kaynak metali mukavemeti ana metalden

Received: 28/01/2025, Revised: 01/05/2025, Accepted: 07/05/2025

daha düşük olduğu tespit edilmiştir. Birleştirmelerde en düşük sertlik değerlerinin, ITAB yumuşaması nedeniyle ana metale yakın ITAB bölgesinde oluştuğu tespit edilmiştir.

Anahtar Kelimeler: Ramor 500 zırh çeliği, GMAK, kaynaklanabilirlik, mekanik özellikler, kırılma türü

I. INTRODUCTION

To provide ballistic protection levels expected from armor steels used in military applications, it is very important that the production methods of armored vehicles are determined during the design stage. For this purpose, the desired protection levels should be provided by using advanced testing and verification methods [1, 2]. In the case of armor steels, the main alloying additives are chromium (Cr), nickel (Ni) and molybdenum (Mo) [3]. Armor steels manufactured in accordance with military standards provide ballistic resistance against 7.62, 12.7, 14.5- and 20-mm caliber ammunition [4, 5]. Armor steel grades are classified as heat treatable medium carbon steels, which are strengthened by conventional quenching and tempering (Q&T) [6]. Q&T steels require higher strength, good toughness and high hardness [7, 8]. Armor steel microstructures are composed of tempered martensite or bainite, depending on the heat-treatment process [9].

In the manufacturing industry there is also a need to join the armor steel used especially in armored vehicle production. Armor steels are susceptible to hydrogen induced cracking (HIC) after welding and they exhibit HAZ softening which cause weak ballistic properties [10, 11]. The Gas Metal Arc Welding (GMAW) is frequently used among the methods for joining armor steels. GMAW is a process that involves heating, melting, and solidifying the base metals and filler metal within a confined fusion zone, using a transient heat source to create a bond between the base metals [12]. The continuous wire electrode is supplied by an automatic wire feeder and passes through the contact tip in the welding torch, where it melts due to internal resistive power and heat transferred from the welding arc. The GMAW welding parameters such as heat input influence the quality, productivity, and cost of the weld joint [13].

In the literature, there are studies on welded joints of armor steels. In one of these studies, Balakrishnan et al [14] investigated the welded joint of quenched and tempered AISI 4340 steels, which is known to have superior ballistic performances and is therefore used in the production of armored vehicles. They determined that the strength of the welded joint, relative to the base metal, decreased because of welding thermal cycling [14]. Soy et al [15] determined the arc welding parameters for armor steels using gas shielded metal arc welding method in their study. A welding simulator was developed and used in a computer program for the determined welding parameters, selected welding technique, material thickness and welding position [15]. Kara and Korkut [16] joined Ramor 500 armor steel couple with MIG welding method in different weld bead geometries. Effects of weld bead geometries on the mechanical and metallurgical properties of weldment is investigated in detail. Gunen et al [6], joined Ramor 500 steels with different welding methods (cold-metal transfer arc weld, GMAW and hybridplasma arc weld) and compared the mechanical properties of the weldments. Robledo et al [17] joined armor steel which produced in accordance with MIL-A-46100 military standard, with GMAW developed a new welding procedure. They pointed out that a narrower HAZ was formed in the newly developed procedure compared to the previous methods. In addition, higher toughness values were achieved in the weldment. The results confirm that this new procedure is a suitable alternative for welding MIL-A-46100 armor steel [17]. Magudeeswaran et al [18] compared the effect of two different consumables (E307 stainless-steel and E11018 steel) in GMAW of quenched and tempered steels. They reported that the joints produced with E11018 weld filler metal showed 13% better fatigue properties than the weldments produced using conventional E307 weld consumables [18]. Findings in the literature indicate that the mechanical properties of armor steels are significantly affected by the microstructural transformation and grain size changes that occur in welded joints due to the weld thermal cycle. To obtain a joint free from weld defects and the risk of crack formation, the basic properties of the base metal must be known. The factors affecting the weldability of steels are the chemical composition, carbon equivalent (Ceq), metallurgical and physical properties of base metal, welding method used,

filler metals and type, weld geometry, pre-heat, heat input and post weld heat treatments [19]. In arc welded joints of armor steels, the structure formed by the transformations in the weld metal and HAZ significantly affects the mechanical properties. Previous studies conducted with MIG or GMAW highlight the significant effects of welding parameters on the mechanical properties of armor steels.

Research indicates that there is a lack of study on the GMAW capability of Ramor 500 quality steel, an important member of the armor steel family, and the effect of microstructure transformation in the weld metal and HAZ according to the welding thermal cycle on the mechanical properties of the joint. Therefore, it was aimed to investigate the GMAW capability of Ramor 500 armor steels used in the military defense industry. For this purpose, Ramor 500 armor steel couples were joined with automatic GMAW at optimized welding parameters determined by preliminary experimental tests. The welded sample was subjected to a radiographic examination with X-ray diffraction, one of the non-destructive testing methods, to check if there were any defects in the weld. Tensile, bending and Charpy-Vnotch impact tests were performed to determine the mechanical properties of the welds. Transverse and vertical microhardness measurements were made along the weld cross-section. In addition, the fracture surfaces of the tensile test samples were examined by SEM-EDS analysis.

II. EXPERIMENTAL METHOD AND MATERIAL

In the experimental studies, 6.5 mm thick Ramor 500 armor steel plates were used. The spectral analysis of the metal used in the study was performed and its chemical composition is given in Table 1.

Base metal	С	P	Mn	Si	S	Ni	Cr	Mo	В	Cu	Fe
	(%)	(%)	(%)	(%)	(%)	(%)	(%)	(%)	(%)	(%)	(%)
Ramor 500	0.35	0.01	1.5	0.7	0.00	1.8	1.00	0.65	0.003	-	Bal.

Table 1. Chemical composition of Ramor 500 armor steel.

The Ramor 500 steels, extensively utilized for defense applications against high-velocity impacts, were selected for this study. They are not intended for further heat treatment because of delivered in quenched condition [20, 21]. The plates with dimensions of $100x400x6.5 \text{ mm}^3$ were joined by automated GMAW method. In the welding process, an automated EWM AG Phoneix 452 plus MM C type MIG / MAG welding machine with TMD5X5KOLON-BOM was used. Before starting welding, welding positioning was set up and then the process parameters determined by pre-experimental studies were entered into the computer part of the machine and then welding process was started. In the welding process, a camera was used to follow the welding nozzle. The water-cooling welding torch was used to weld with both gas protection and filler metal. The weld width was adjusted by the torch's oscillation movement unit integrated by a computer. The automated welding machine and filler metal feeding unit are shown in Figure 1.

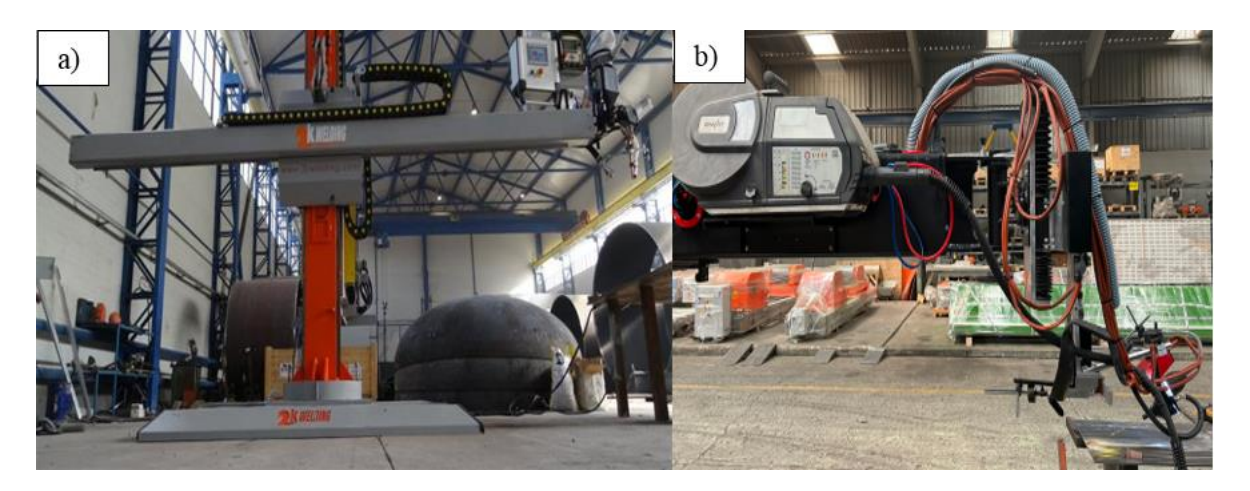


Figure 1. a) Automated welding machine with column-boom system and b) filler metal feeding unit

The welding parameters used for joining were determined by pre-experiment given in Table 2. The V shaped grooved plates were joined in the horizontal position (PA) by automated (robot) GMAW using filler metal. After the first pass, the second pass weld bead was performed from root side (Figure 2). ER 110 SG coded filler metal with a diameter of 1.2 mm was used in the joining. The chemical compositions of the used filler metal obtained from the catalog are 0.09% C, 1.7%Mn, 0.75% Si, 2% Ni, 0.3%Cr, 0.5%Mo, 0.2% Cu and the rest Fe. The chemical composition of the shielding gas used during welding is 86% argon, 12% carbon dioxide and 2% oxygen.

Material		Voltage (V)	Current (A)	Wire Speed (m/dk)	Welding speed (cm/dk)	Heat input (kJ/mm)
Ramor	Plate-1-2 cap			5.5		0.871
500	Plate-1-2 root	21	190	6.0	22	0.871

Table 2. Automated GMAW process parameters

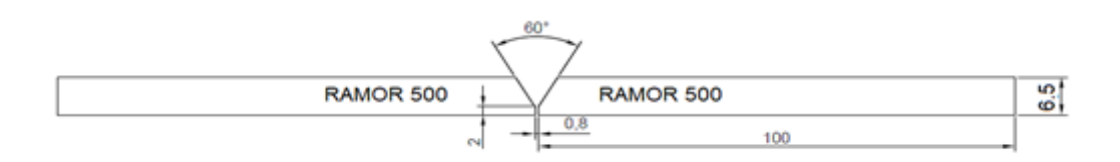


Figure 2. Welding position.

Radiographic tests were carried out by X-ray method for weldment according to EN ISO-17636-1:2013 standard. The test was carried out with the Radiographic Test Device of PARS Quality Company. For the tensile tests, two samples of Ramor 500 base metal were prepared according to TS EN ISO 6892-1 standard and two samples of Ramor 500 welded joints were prepared according to TS EN ISO 4136 standard. Tensile test was performed at UMT Quality Control Eng. in the longitudinal direction at a tensile test machine of UTEST brand UTC-4870 model with a capacity of 600 kN at with speed of 10 mm/min. For the bending test, two specimens were prepared according to the process parameters in accordance with TS EN ISO 7438. The bending test was performed at a compression speed of 2 mm/min on a Zwick/Roell Z600 brand/model bending test machine capable of applying a load of 600 kN. For the determination of Charpy-notch impact properties of samples, two test specimens (substandard specimen 6.5x10x55 mm³) fabricated. Notch impact tests were carried out at room temperature (20°C)

on a Zwick/Roell Rkp450 brand/model notch impact test machine with an impact energy application capacity of 450 Joules. In addition, the fracture surface images formed after the tensile tests were examined with a Zeiss Ultra Plus brand Scanning Electron Microscope (SEM). For metallographic investigation and HAZ width measurement of the weldment, the samples grinding with 250-1800 grit abrasive SiC papers and then polished. The weldments were etched using a 2% Nital for 5-6 s. Metallographic evaluations were conducted using a Nikon 200 optical microscope. Microhardness measurements were performed along the weld cap and root line, including the base metal, HAZ and weld metal. Tests were performed on a QNESS Q250M Vickers hardness tester with 500 g load. The experimental test samples obtained from the welded joints are schematically shown in Figure 3.

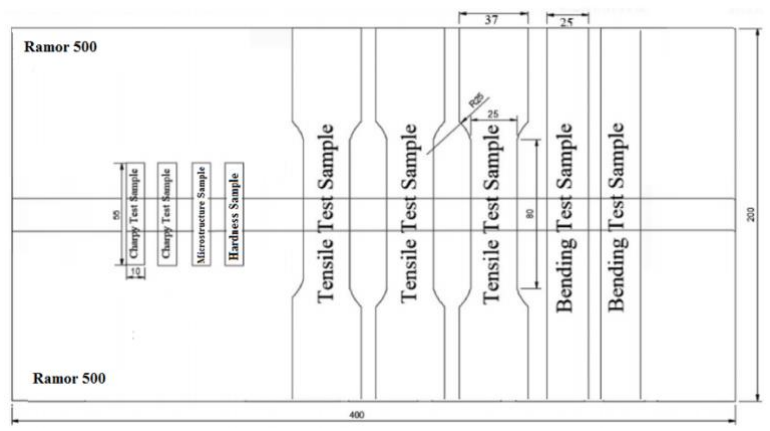


Figure 3. Schematic representation of the experimental samples.

III. EXPERIMENTAL RESULTS

A. RESULTS OF RADIOGRAPHIC EXAMINATION

The radiographic inspection image conducted to determine whether the joint contains weld defect is shared in Figure 4.



Figure 4. X-ray radiographic inspection results of Ramor 500 armor steel weldment.

Inspection result confirms that the GMAW process was successful, as no defects were detected in the weld.

B. TENSILE TEST RESULTS

The average yield, tensile strength, and elongation % of the base metal and weldment are given in Table 3. In addition, stress - % elongation curves and fracture images are shown in Figure 5.

Table 3. Tensile test results of base metal and weldment

		Average Yield Strength (MPa)	Average Tensile Strength (MPa)	Average % Elongation	Fracture Result
Ra	amor 500 base metal	1587	1665	8.2	Fractured base metal
	Weldment	907	976	4.1	Weld metal

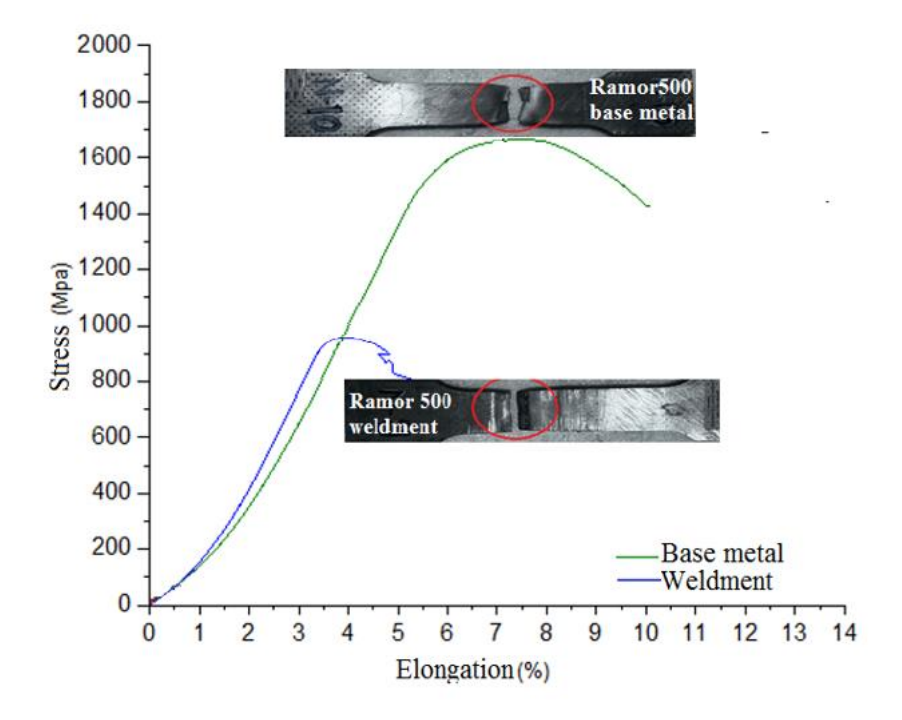


Figure 5. Tensile test graphs and fracture images of Ramor 500 base metal and weldment

As seen in Table 3 and Figure 4, the average yield strength, tensile strength and % elongation of base metal was 1587 MPa, 1665 MPa and 10.1%. However, they were determined as 976 MPa, 907 MPa and 5.1% respectively for GMAW sample. Results indicate that there is a decrease in the strength and ductility of the weldment as compared to the base metal. Since armor steels have been subjected to quenching & tempering conditions during production, strength and ductility of the weldment has adversely affected because of transformation and grain size variation related with weld thermal cycle. Although these steels with good weldability undergo structural transformation due to the weld thermal cycle and softening may occur in the HAZ so, decrease in tensile and fatigue strength [22-24]. Tensile test sample of weldment fractured from the weld metal (Figure 5). The fracture surface of samples was examined SEM and the EDS analysis was performed. Analysis results are shown in Figure 6.

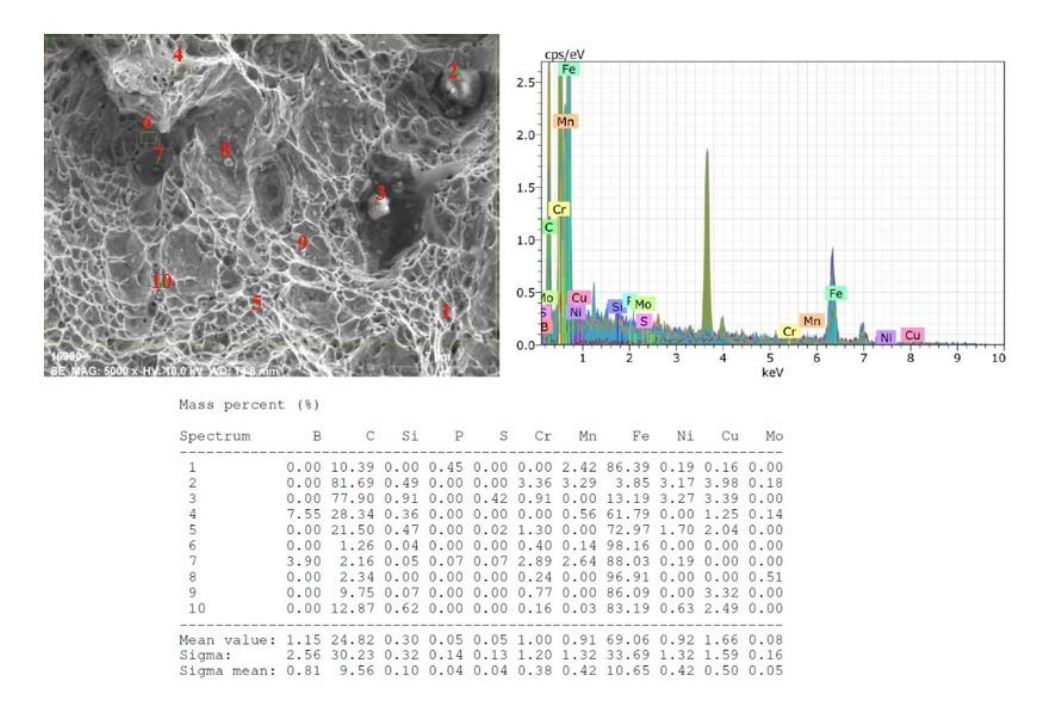


Figure 6. EDS result carried out from the fracture surface of Ramor 500 armor steel

The formation of the honeycomb-like dimple structures in the surface indicates that welded sample intergranular fractured in a ductile mode. However, the local transgranular cleavage plane in some grains also indicates that sample fractured in a semi-ductile/semi-brittle mode. The results of point EDS analysis indicate that the increase in the amount of carbon, chromium, nickel and manganese and the decrease in the amount of iron may indicate that other fine carbides as well as cementite may form in the weld metal. These precipitates which are harder than the matrix, contribute to the formation of crack initiation. Alipooramirabad et al. [25] similarly reported the presence of very fine carbide precipitates in armor steels. Taşkaya et al [26] examined the fracture surface images of Ramor 500 steels joined by SAW method and reported that the tensile test specimens fractured in a ductile type and carbide precipitates occurred in the structure after XRD analysis. In another study, the presence of needle-shaped ε -Fe2.4C carbides with a hexagonal lattice was similarly detected in quenched 0.17C-1.5Mn-B steel produced in the form of Q&T and similar carbides were detected by TEM microscopy [27, 28]. It was also stated that due to the presence of a sufficient amount of Mo (2.0%) in the structure, it can form fine needle-shaped M₂C-type carbide precipitates together with Cr [29].

C. CHARPY-V NOTCH IMPACT TEST RESULT

The toughness of base metal and weldment at room temperature was determined by Charpy V-Noch test. Results are given in Table 4.

Table 4. Charpy V-notch impact test data for Ramor 500 armor steels and weldment.

Sample	Charpy V-Notch Impact Strength (J) (+20 °C, room temperature)			
Ramor 500 base metal	32.3 ± 2			
Ramor 500 weldment	62.8± 2			

The toughness of Ramor 500 base metal and weldment was found 32.3J and 62.8J respectively. The weld metal impact strength increased as compared to the base metal due to microstructural transformation in the weld metal related to the weld thermal cycle. Normally Q&T armor steels contain hard tempered lath martensite in the microstructure [30]. The tempered hard martensitic structure that forms the structure of the base metal can be evaluated as the reason for the increase in toughness by transforming into softer phases in the weld metal because of welding thermal cycle. The decrease in the elongation obtained in the tensile test process compared to the base metal may be related to the hard precipitates in the structure creating the beginning of fracture. It is stated that four times higher toughness is obtained in Ramor 500 armor steel GMAW joints compared to the base metal [31].

D. BENDING TEST RESULTS

The formability of the welded joint was also determined by three-point bending test. The bending strength of weldment is given in Table 5. The bending force - deformation curves and the region where cracking occurred is shown in is shown in Figure 7. The three-point bending test was performed by applying load to one sample from the weld surface and to the other sample from the weld root.

Sample	Max. Bending Angle (°)	F _{max} (N)	dL at Fmax (mm)	a ₀ (Thickness) (mm)	b ₀ (Width) (mm)	S ₀ (Area) (mm)
Weld face	90	15611.44	18.82162	6.75	19.5	131.625
Weld root	90	18711.74	23.71527	6.77	19.58	132.5566
Average	-	17161.59	-	-	-	-

Table 5. Bending test data for Ramor 500 armor steel weldments.

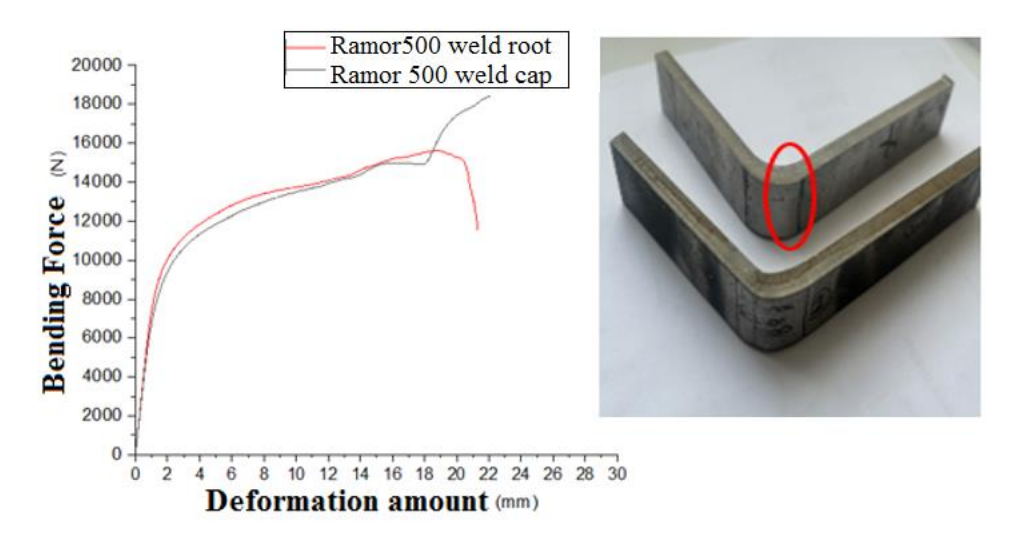


Figure 7. The bending force - deformation curves and tested welded sample.

Both welded samples subjected to bending tests cracked after being shaped at approximately 90°. In the sample where the load was applied from the weld root, the crack formation occurred in the HAZ, and in the sample where the load was applied from the weld cap, it occurred in the weld metal. It is thought that local softening in the HAZ contributed to this crack formation.

E. MICROSTRUCTURE INVESTIGATION AND MICROHARDNESS RESULTS

The hardness distribution of the cross-sectional direction and weld center line from weld cap to root of weldment are shown in Figure 8 a and b.

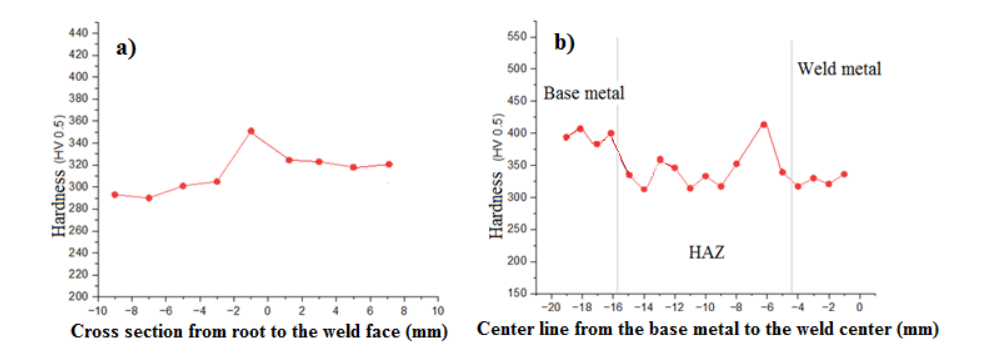


Figure 8. Hardness values taken along a) in the weld metal center line from weld cap to root b) on the cross section covering base material, HAZ and weld metal.

The microstructures of Ramor 500 armor steel weldment are, shown in Figure 9, examined to evaluate the relationship between mechanical properties and microstructure of the weldment.

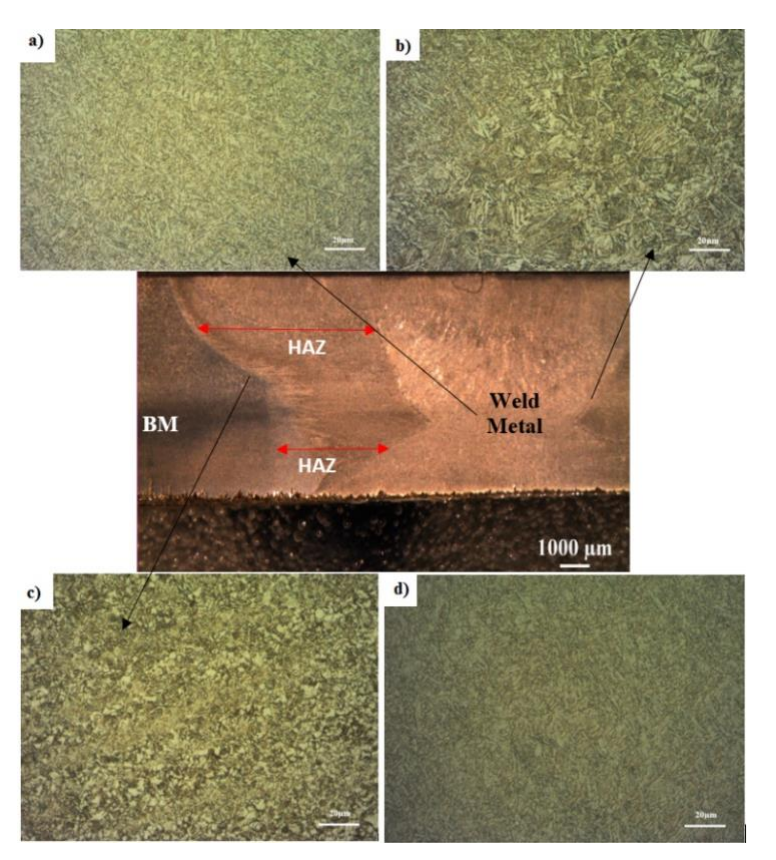


Figure 9. The microstructure of Ramor 500 weldment, a) weld metal, b) weld metal-HAZ transition zone, c)

Haz-base metal transition zone, d) base metal

As seen from Figure 8a, there is an increase in the hardness of the weld metal from the weld root to the weld cap. It was determined that the weld metal hardness varies between 290 HV and 350 HV. The decrease in hardness at the weld root is related to the tempering heat treatment effect of the second seam applied by the weld root to the root side of the first seam during the joining process. As Fig 8b, hardness

of the base metal is 405 HV. It slightly decreased in the partially transformed region of HAZ due to microstructural transformation, grain size coarsening and local softening. The local softening is related to annealing or transformation, where the temperature of the weld thermal cycle reached is below A₁, this is known annealing softening. Due to tempering processes, which are generally carried out below A₁ temperature, in the HAZ of weldment cause carbon rejection of the supersaturated martensite phase and transformation of metastable carbides into stable ones or spheroidization of carbides so, softening [32-34]. However, in the coarse-grained region of HAZ, it determines the highest hardness values of weldment. Similar results reported by Son et al [35]. The higher hardness values in this region of the HAZ compared to the weld metal and the base metal can be attributed to the formation of hard phases such as martensite. The average weld metal hardness was determined as 305 HV because of structural transformation. The decrease in strength of the welded joint supports this. The reason for the low formability as well as strength of the weld metal is the increase in hardness in the coarse-grained region of the HAZ.

Fig. 9 shows microstructure of the weldment covering BM. (base metal), HAZ and the WM, (weld metal). Fig.9a shows the WM of the welded sample mainly decorated by lath martensite in ferrite, columnar grains. The grain growth occurs in the coarse grain region of HAZ next to the fusion line (weld metal-HAZ transition) (Fig. 9b). Moving from weld metal towards the base metal, the HAZ microstructure changes significantly. Fig. 9c shows the microstructure in the HAZ near the base metal (HAZ-base metal transition) consists of tempered lath martensite, bainite and ferrite phases. Skowronska et al [36] confirms that there is completely tempered martensite with visible boundaries of the former austenite grains on which granular ferrite was formed in this area. As seen Fig.9d, base metal microstructure consists of tempered lath martensite [37].

It is determined that the HAZ width of the weldment is much wider near the weld cap and decreases gradually towards the weld root. The grain coarsening in HAZ and local softening occurred on the partially transformed region of HAZ which is next to the base metal. By minimizing heat input and narrowing the HAZ, it effectively reduces grain coarsening and localized softening so, enhances the material's mechanical properties. On the other hand, a wide HAZ formation may also be beneficial for welding steels that are susceptible to martensite formation [6]. The larger width of the softening zone leads to a decrease in the hardness and the mechanical properties of Ramor500 joints compared to the base metal. The width of the HAZ was within the range accepted by the MIL-STAN-1185 standard, (maximum 15.9mm from the centerline of the joint). Ramor 500 weldments exhibit tensile strength values that are lower than those of the base metal. A reduction in the mechanical properties of a weldment is usually associated with softening or grain coarsening, especially at the weld metal or HAZ [6, 38, 39].

IV. CONCLUSION

Ramor 500 steel, which is frequently used in the production of armored military vehicles, was joined using the GMAK method. In the study where the mechanical and metallurgical properties of the joining were investigated on a large scale, the following findings were obtained.

- Radiographic examinations confirm that the Ramor 500 steel pair was successfully joined using the robotic GMAK method, free from welding defects.
- Although the strength of the welded joint tested under the effect of static load was found to be lower than the base material, it was found to be within the acceptable range since it provided 2/3 of the strength of the base metal. It was determined that the joint damaged by the weld metal broke with a semi-ductile-semi-brittle fracture mode. It is thought that the hard metal carbides detected in the weld metal contributed to the initiation of fracture.

- Due to the softer phases formed in the microstructure of the weld metal compared to the base metal, the impact absorption energy of the joint was found to be approximately 35 J higher than that of the base metal formed in the structure.
- In the bending test process carried out with the loading applied from the weld surface and root, it was determined that the welded joints cracked from the weld metal and HAZ after being shaped at 90°. It is believed that the crack formation is affected by the crack initiation of the carbides formed in the weld metal and the hard phase such as martensite formed in the HAZ.
- The hardness increase from the weld root to the weld cap was determined in the weld centerline. It is believed that the hardness decrease in the weld root is due to the heat treatment effect on the first weld seam weld made from the back side of the weld workpiece. In the hardness measurement covering the base metal, HAZ and weld metal, a significant decrease in hardness was detected as the weld progressed from the base metal to the weld metal except for the HAZ coarse-grained region. The martensitic structure of the base metal underwent structural transformation so, the formation of softer phases is responsible for the decrease in hardness. In addition, it was determined that regional softening occurred in the part of the HAZ close to the base metal.
- The width of the HAZ was within the range accepted by the MIL-STAN-1185 standard, (max. 15.9 mm from the centerline of the joint).

Article Information

Acknowledgments: The authors would like to express their sincere thanks to the editor and the anonymous reviewers for their helpful comments and suggestions.

Author's Contributions: Writing—original draft, H.E.E. and R.K, writing—review, analysis and editing, H.E.E, S.K. and R.K. All authors have read and approved the final version of it.

Artificial Intelligence Statement: No any Artificial Intelligence tool is used in this paper.

Conflict of Interest Disclosure: No potential conflict of interest was declared by authors.

Plagiarism Statement: This article was scanned by the plagiarism program.

V. REFERENCES

- [1] Military Specification: Armor Plate, Steel, Wrought, Homogeneous (For Use In Combat-Vehicles And For Ammunition Testing), MIL-A-12560H, US Military: Watertown, MA, USA, 2007.
- [2] Armor Plate, Steel, Wrought, High-Hardness, MIL-A-46100E, U.S. Military Specification, 2008.
- [3] E. R. S. Souza, R. P. Weber, S. N. Monteiro and S. D. S. Oliveira, "Microstructure effect of heat input on ballistic performance of welded high strength armor steel," *Materials*, vol. 14, 2021, Art. no. 5789.
- [4] S. J. Manganello and A. D. Wilson, "Direct quenching and its effects on high-strength armor plate," in *International symposium on low-carbon steels for the 90's*, R. Asfahani and G. Tither, Eds. The Minerals, Metals & Materials Society, Pittsburgh, USA, 1993, pp. 235-241.
- [5] F. Ade, "Ballistic qualification of armor steel weldments," *Welding Journal*, vol. 70, pp. 53-58, 1991.

- [6] A. Günen, S. Bayar and M. S. Karakaş, "Effect of different arc welding processes on the metallurgical and mechanical properties of Ramor 500 armor steel," *Journal of Engineering Materials and Technology*, vol. 142, no. 2, 2019, Art. no. 021007.
- [7] M. Balakrishnan, V. Balasubramanian and G. M. Reddy, "Effect of hardfaced interlayer thickness on ballistic performance of armour steel welds," *Materials and Design*, vol. 44, pp. 59–68, 2013.
- [8] T. Özdemir, "Mechanical & microstructural analysis of armor steel welded joints," *International Journal of Engineering Research and Development UMAGD*, vol. 12, no. 1, pp. 166-175, 2020.
- [9] J. Prifti, M. Castro, R. Squillacioti and R. Cellitti, "Improved rolled homogeneous armor (IRHA) steel through higher hardness," U.S. Army Research Laboratory, Aberdeen Proving Ground, USA, ARL-TR-1347, 1997.
- [10] P. V. Ramana, G. M. Reddy and T. Mohandas, "Stress distribution in high strength low alloy steel weldments," *Journal of Non Destructive Testing and Evaluation (JNDE)*, vol. 6, pp. 33–40, 2007.
- [11] G. Magudeeswaran et al., "Influences of flux-cored arc welding consumables on dynamic fracture toughness of armour grade Q&T steel joints," *Fatigue Fracture Engineering Materials and Structures*, vol. 32, pp. 587–600, 2009.
- [12] H. R. Ghazvinlo, A. Honarbakhsh and N. Shadfar, "Effect of arc voltage, welding current and welding speed on fatigue life, impact energy and bead penetration of AA6061 joints produced by robotic MIG welding," *Indian Journal of Science and Technology*, vol. 3, no. 2, pp. 156-162, 2010.
- [13] I. A. Ibrahim, S. A. Mohamat, A. Amir and A. Ghalib, "The effect of gas metal arc welding (GMAW) processes on different welding parameters," *Procedia Engineering*, vol. 41, pp. 1502 1506, 2012.
- [14] M. Balakrishnan, V. Balasubramanian, R. G. Madhusuhan and K. Sivakumar, "Effect of buttering and hardfacing on ballistic performance of shielded metal," *Materials & Design*, vol. 32, no. 2, pp. 469-479, 2011.
- [15] U. Soy, O. Iyibilgin, F. Findik, C. Oz and Y. Kıyan, "Determination of welding parameters for shielded metal arc welding," *Scientific Research and Essays*, vol. 6, no. 15, pp. 3153-3160, 2011.
- [16] S. Kara and M. H. Korkut, "Zırh çeliklerinde kaynak ağzı tasarımının metalurjik ve mekanik özelliklere etkisinin araştırılması," *Makine Teknolojileri Elektronik Dergisi*, vol. 9, no. 1, pp. 35-45, 2012.
- [17] D. M. Robledo, J. A. A. Gómez and J. E. G. Barrada, "Development of a welding procedure for MII A 46100 armor steel joints using gas metal arc welding," *National University of Colombia*, vol. 168, pp. 65-71, 2010.
- [18] G. Magudeeswaran, V. Balasubramanian and G. M. Reddy, "Hydrogen induced cold cracking studies on armour grade high strength, quenched and tempered steel weldments," *International Journal of Hydrogen Energy*, vol. 33, pp. 1897–1908, 2008.
- [19] M. Vural, F. Piroğlu, Ö. B. Çağlayan and E. Uzgider, "Yapı çeliklerinin kaynaklanabilirliği," *TMH Türkiye Mühendislik Haberleri*, vol. 4, no. 426, pp. 47-51, 2003.
- [20] Ramor 500 Armor Steel Data sheet 2033 Ramor 500 2017-04-19, SSAB. [Online] Available. https://www.ssab.com/en/brands-and-products/armox/product-offer/ramor-500.

- [21] M. L. Bekci, B. H. Canpolat, E. Usta, M. S. Güler and Ö. N. Cor, "Ballistic performances of Ramor 500 and Ramor 550 armor steels at mono and bilayered plate configurations," *Engineering Science and Technology, an International Journal*, vol. 24, no. 4, pp. 990-995, 2021.
- [22] F. Falkenreck, A. Kromm and T. Böllinghaus, "Investigation of physically simulated weld HAZ and CCT diagram of HSLA armour steel," *Welding World*, vol. 62, pp. 47-54, 2018.
- [23] F. Hochhauser, W. Ernst, R. Rauch, R. Vallant and N. Enzinger, "Influence of the soft zone on the strength of welded modern HSLA steels," *Welding World*, vol. 85, pp. 77-85, 2012.
- [24] B. Hanhold, S. S. Babu and G. Cola, "Investigation of heat affected zone softening in armour steels Part 1—Phase transformation kinetics," *Science and Technology of Welding & Joining*, vol. 18, pp. 247-252, 2013.
- [25] H. Alipooramirabad, A. Paradowska, M. Reid and R. Ghomashchi, "Effects of PWHT on the residual stress and microstructure of Bisalloy 80 steel welds," *Metals*, vol. 12, no. 10, 2022, pp. 1569.
- [26] S. Taşkaya and A. K. Gür, "Investigation of the equilibrium of permeate in the welding speed of the wire feeding speed in joining Ramor 500 armor steel with submerged arc welding method," *Gümüşhane University Journal of Science and Technology*, vol. 9, no. 3, pp. 444-453, 2019.
- [27] G. Magudeeswaran, V. Balasubramanian and G. M. Reddy, "Metallurgical characteristics of armour steel welded joints used for combat vehicle construction," *Defense Technology*, vol. 14, pp. 590–606, 2018.
- [28] Z. Fei, D. Pan, H. Cuiuri Li and A. A. Gazder, "A combination of keyhole GTAW with a trapezoidal interlayer: a new insight into armour steel welding," *Materials*, vol. 12, 2019, Art. no. 3571.
- [29] D. Tomerlin, D. Mari, D. Kozak and I. Samardži', "Post-weld heat treatment of S690QL1 steel welded joints: influence on microstructure, mechanical properties and residual stress," *Metals*, vol. 13, no. 5, 2023, Art. no. 999.
- [30] S. Bakhshi and A. Mirak, "Textural development, martensite lath formation and mechanical properties variation of a super strength AISI4340 steel due to austenitization and tempering temperature changes," *Materials Characterization*, vol. 188, 2022, Art. no. 111923.
- [31] A. Cabrilo and K. Geric, "Fracture mechanic and charpy impact properties of a crack in weld metal, HAZ and base metal of welded armor steel," *Procedia Structural Integrity*, vol. 13, pp. 2059-2064, 2018.
- [32] M. S. Khan, M. Soleimani, A. R. H. Midawi, I. Aderibigbe, Y. N. Zhou and E. Biro, "A review on heat affected zone softening of dual-phase steels during laser welding," *Journal of Manufacturing Processes*, vol. 102, pp. 663–684, 2023.
- [33] L. Morsdorf, E. Emelina, B. Gault, M. Herbig and C. C. Tasan, "Carbon redistribution in quenched and tempered lath martensite," *Acta Materialia*, vol. 205, 2020, Art. no. 116521.
- [34] H. Ertek Emre, S. Keçe and R. Kaçar, "The effect of PWHT on the mechanical properties of HHA 500 armor steel welds," *Proceedings of the Institution of Mechanical Engineers, Part E: Journal of Process Mechanical Engineering*, early access, Feb 11, 2025, doi:10.1177/09544089251318111.
- [35] H. J. Son, Y. C. Jeong, B. W. Seo, S. T. Hong, Y.-C. Kim and Y. T. Cho, "Weld quality analysis of high-hardness armored steel in pulsed gas metal arc welding," *Metals*, vol. 13, 2023, Art. no. 303, 2023.

- [36] B. Skowrońska, J. Szulc, M. Bober, M. Baranowski and T. Chmielewski, "Selected properties of Ramor 500 steel welded joints by hybrid PTA-MAG," *Journal of Advanced Joining Processes*, vol. 5, 2022, Art. no. 100111.
- [37] Z. Fei et al., "Investigation into the viability of K-TIG for joining armour grade quenched and tempered steel," *Journal of Manufacturing Processes*, vol. 32, pp. 482-493, 2018.
- [38] G. Magudeeswaran, V. Balasubramanian, T. S. Balasubramanian and G. M. Reddy, "Effect of welding consumables on tensile and impact properties of shielded metal arc welded high strength, quenched and tempered steel joints," *Science and Technology of Welding and Joining*, vol. 13, pp. 97-105, 2008.
- [39] A. Saxena, A. Kumaraswamy, G. M. Reddy and V. Madhu, "Influence of welding consumables on tensile and impact properties of multi-pass SMAW Armox 500T steel joints vis-a-vis base metal," *Defence Technology*, vol. 14, pp. 188-195, 2018.